

# The relationship between the extent of indentation and impact damage in carbon-fibre reinforced-plastic composites after a low-velocity impact

R.A. Brooks<sup>1a</sup>, J. Liu<sup>1</sup>, Z.E.C. Hall<sup>1</sup>, A.M. Joesbury<sup>2</sup>, L.T. Harper<sup>2</sup>,  
H. Liu<sup>3</sup>, A.J. Kinloch<sup>1</sup> and J.P. Dear<sup>1a</sup>

<sup>1</sup>Department of Mechanical Engineering, Imperial College London, Exhibition Road, London, SW7 2AZ, UK,

<sup>2</sup>Composites Research Group, University of Nottingham, University Park, Nottingham, NG7 2RD, UK

<sup>3</sup>School of Engineering and Materials Science, Queen Mary University of London, Mile End Road, London, E1 4NS, UK

<sup>a</sup>Corresponding authors: [richard.brooks16@imperial.ac.uk](mailto:richard.brooks16@imperial.ac.uk) and [j.dear@imperial.ac.uk](mailto:j.dear@imperial.ac.uk)

## Abstract

The present paper investigates the low-velocity impact behaviour of carbon-fibre reinforced-plastic (CFRP) composite panels and the damage incurred when they are subjected to a single impact. The relationship between the depth of permanent surface indentation that results and the associated area of interlaminar delamination damage is investigated for two different thicknesses of composite panels. In particular, the delamination damage area increases with impact energy for both thicknesses of composite panel that were studied. Likewise, the indentation depth also increases with increasing impact energy, again for both thicknesses of CFRP panels. It is shown that the indentation depth, at the centre of the indentation, may be used to provide an indication of the extent of delamination damage within the CFRP panel after impact. Indeed, from plotting the indentation depth versus the interlaminar delamination normalised by the thickness of the panel area there is shown to be a unique 'master' relationship, with a positive intercept indicating that the indentation damage seems to result before delamination damage initiates. Thus, for both thicknesses of CFRP panels, it is suggested that the indentation process is a precursor to interlaminar delamination damage.

**Keywords:** CFRP composite; impact behaviour; indentation damage; delamination damage

## 1. Introduction

Lightweight composite materials, in particular carbon-fibre reinforced-plastic (CFRP) materials, have been replacing metals in certain applications in the aerospace industry. Advantageous properties, such as their high strength-to-weight ratio and good fatigue resistance, make the adoption of these composite materials desirable. In particular, the need to reduce emissions has driven the development of these materials within the aerospace, and other, industries. Also, clearly, the cost savings associated with the improved fuel efficiency acts as a further incentive to adopt CFRP composites.

However, one area of concern regarding the use of CFRPs as part of an aircraft's structure is their impact performance. Impact events may occur due to the dropping of tools during maintenance, bird strikes, runway debris, hailstones or through collisions with airport vehicles. Depending on the velocity of the impacting object, these impact events can be categorised into low-velocity and high-velocity impacts. Vaidya [1] defined an upper boundary for low-velocity impacts of about  $10 \text{ m.s}^{-1}$  based upon how a target responds during an impact. During low-velocity impacts, the contact time between the impactor and target is relatively long, allowing the target to absorb the impact energy through elastic deformation, damage formation and vibration [2]. Upon reaching a maximum displacement, the elastic energy stored in the target starts to cause the impactor to rebound. In contrast, high-velocity impact causes a more localised response in the target, dissipating energy over a comparatively smaller region [2]. The current research focuses on low-velocity impacts.

Although damage induced from an impact may not be easily visible from the surface, and thus is known as 'barely visible impact damage' (BVID), such damage can weaken the structure. Furthermore, if left unrepaired, this damage may be increased in extent by fatigue stresses, or even further impacts. This can lead to catastrophic failure if the residual strength or the strength of the structure falls beneath the working load. Therefore, relatively small permanent indentations on a composite surface could be an indicator of major internal damage and/or the precursor to major internal damage developing later in the service-life of the CFRP component.

Permanent surface indentations after impact loading of a range of very different materials have interested researchers for at least the last 75 years. Hutchings [3] has quoted the work of Tabor who showed that the process of indentation during impact requires yielding and plastic flow of the impacted material to occur and that the volume of the remaining permanent indentation was directly related to the difference between the impact energy and the rebound energy of the impacting body, assuming that the impactor did not deform in the

impact event. Tabor studied mostly metals and clearly showed that there was a threshold for these indentation processes determined by the plastic behaviour of the metal.

For composite materials, Wardle and Lagace [4] were some of the first researchers to link the indentation damage to the interlaminar delamination and intralaminar (e.g. matrix cracking and fibre debonding and fracture) damage and demonstrated that they were physically related. Shi et al. [5] showed that it was the absorption during the impact event of the initial impact energy which was key in determining these various damage processes. In particular, Wagih et al. [6] showed clearly that indentation in the composite material is often a pre-requisite for intralaminar and interlaminar delamination damage. Wardle and Lagace [4] found that for plate and shell structures, with thicknesses less than 2.4 mm, no correlation was found between the indentation depth and internal damage that occurred. However, Komorowski et al. [7] reported a clear correlation between the indentation depth and the area of the interlaminar delamination damage for CFRP panels ranging from 8 to 48 plies in thickness. Notwithstanding, Talreja and Phan [8] have suggested that the indentation depth may be affected by the strength and toughness of only the surface ply of the impacted CFRP. Thus, they considered that the claim that the entire indentation depth was associated with the impact-induced damage within the CFRP was not substantiated. Indeed, the suggestion that the indentation depth may be correlated with interlaminar or intralaminar cracks within the CFRP laminate, and is indicative of the incident impact energy, has to date not been completely supported by analysis or experiments [8]. Further, Vieille et al. [9] observed a higher extent of permanent indentation in thermoplastic-matrix CFRPs (i.e. CF/Polyether-ether ketone and CF/Polyphenylene sulphide) compared to a thermosetting-matrix CFRP (i.e. CF/Epoxy). On the other hand, Leicy and Hogg [10] observed only a relatively small indentation depth, on the impacted face, for the thermoplastic-matrix CFRPs after a low-velocity impact, leading to a dome forming on the rear tensile surface at higher impact energies. Cracking initiated earlier on the rear tensile surface for thermoset-matrix CFRPs and no indentation was observed on the impacted front face. Leicy and Hogg [10] suggested that the initial indentation seen in the thermoplastic-matrix CFRPs could modify the local stresses under the impactor, allowing damage to develop in a more stable manner, compared to the thermoset-matrix CFRPs. Hence, thermoplastic matrices were deemed to be better than thermosetting matrices for energy absorption after total penetration. Shuck, as cited by Talreja and Phan [8], tested woven CF/Epoxy composites with thicknesses of 10, 13 or 16 plies at impact energies below 15 J. As would be expected, the indentation depth increased with an increasing impact energy. Furthermore, 10 ply panels gave a greater indentation depth compared to the 13 and 16 ply panels for the same impact energy. Similarly, Panettieri et al. [11] investigated the indentation depth in quasi-isotropic lay-up CF/Epoxy panels of different

thicknesses. For a laminate of 16 plies, the maximum indentation depth was approximately 0.25 mm at an impact energy of 19.3 J. Whereas, for a 24 ply laminate, a maximum indentation depth of approximately 0.15 mm was measured at an impact energy of 30.5 J. Therefore, from the limited research that has been undertaken into the extent of the indentation depth in impacted composite panels, it appears that thinner panels may sustain a larger indentation depth than thicker panels for a given impact energy but no overall link between the extent of the indentation depth and the extent of interlaminar delamination damage has been established.

The phenomenon responsible for this permanent deformation behaviour is not fully known but multiple potential causes have been suggested. For example, Bouvet et al. [12] have suggested that impact debris accumulating in the intralaminar matrix cracks could prevent the interlaminar delaminations from closing and thus contribute to the extent of the permanent indentation. Other suggestions proposed by Bouvet et al. [12] include the compaction of the matrix polymer, the friction of the delaminated surfaces and the initiation and development of the intralaminar damage modes of matrix cracking and fibre debonding.

In the present work, CF/Epoxy panels of 2.3 and 4.6 mm in thickness are subjected to a central impact with a round-nosed impactor at energies of 2, 5, 10, 15 and 20 J. Load versus time and load versus displacement traces are obtained from the low-velocity drop-weight test that is employed. The indentation depth is measured using two techniques: a handheld digital depth gauge and confocal laser scanning microscopy. This latter technique also provides 3D surface scans from which cross-sections of the indentations may be obtained. Ultrasonic C-scan maps of the interlaminar delamination damage within the CFRP panels are also obtained. Finally, cross-sections of impacted CFRP panels are viewed using optical microscopy to allow identification of the interlaminar and intralaminar cracks. Thus, for the first time, the formation of the surface indentations can be related to (a) the onset of yielding/plasticity in the matrix and matrix cracking of the CFRP, (b) the load versus time trace associated with the impact event and (c) the extent of associated interlaminar delaminations that result.

## **2. Materials and Experimental Methods**

### **2.1. Materials**

The panels of carbon-fibre, with an epoxy matrix, termed CF/Epoxy, were formed using a unidirectional prepreg (MTC510-UD300-HS-33 %RW) supplied by SHD Composites Ltd, UK. This prepreg had a fibre volume fraction of 60% and was laid-up in a quasi-isotropic lay-up of  $[45_2/-45_2/0_2/90_2]_s$  in the case of the 4.6 mm thick panels and in a lay-up of  $[45/-45/0/90]_s$  in the case of the 2.3 mm thick panels. Flat large panels were prepared using an autoclave. A constant pressure of 6 bar was used during curing of the CFRP composite, with a 2°C per

minute temperature ramp up to 110°C where a 120 minute dwell time was used. These larger panels were cut into smaller panels of size 150 mm x 100 mm, with the 0° plies aligned with the longer edge of the panels. The glass transition temperature of the cured CFRP was 133°C.

## 2.2. Experimental methods

Low-velocity drop-weight testing was undertaken in accordance with ASTM Standard D7136 [13] using an Instron CEAST 9340 drop-weight tower, shown in Figure 1, fitted with a hemispherical stainless-steel impactor of diameter 16 mm. This diameter was selected on the basis that previous low-velocity research on the current CFRP indicated that a 16 mm diameter impactor provided a significant delamination damage area at the chosen impact energies, but not too large as to be affected by edge effects. Also, a small yet measurable indentation depth was created, without becoming too concentrated so as to cause penetration. The impactor had an overall mass of 5.27 kg and was dropped from varying heights to give impact energies of 2, 5, 10, 15 or 20 J, with corresponding impact velocities of 0.87, 1.38, 1.95, 2.39 or 2.76 m.s<sup>-1</sup>, respectively. The 150 mm x 100 mm CF/Epoxy panel was clamped onto a steel picture-frame using four rubber-tipped toggle clamps which prevented slippage of the panel during the impact test, see Figure 1. Three guide pins allowed the panel to be aligned centrally under the impactor, above a window cut-out of 125 mm x 75 mm. A load cell located in the forward section of the impactor measured the resulting load versus time data, with a sampling frequency of 500 kHz. Multiple impacts were prevented by an anti-rebound system. The drop-weight tower was connected to a PC equipped with a CEAST DAS 64K data acquisition system, through which the tower was controlled and the data collected. No software filtering was applied to the load versus time data that was outputted and the accompanying software, provided by CEAST, produced both the impact load and resulting displacement of the panel as a function of time for the impact event.

Ultrasonic C-scans were taken following the impact event as a method of non-destructively determining the delamination, i.e. interlaminar, damage area. A portable 'Prisma 16:64 TOFD' ultrasonic C-scan device with a 5 MHz probe, supplied by Sonatest Ltd., UK, was attached to an encoder to allow the position of the probe along the scan axis to be measured. The ultrasonic waves generated are reflected by the delaminations within the CFRP panel and, from this, the transducer can determine the position of the delaminations from the total travel time and the size of the delaminations from the amplitude received by the transducer. Hence, a resulting map of the delamination footprint was produced showing the interlaminar damage at different depths through the panel, with the depths represented by different colours, shown on a scale from 0 to 4.6 mm, or 0 to 2.3 mm, depending on the thickness of the panel. Areas showing no delamination damage are coloured dark blue.

Therefore, by counting the number of pixels which are not dark blue, the total footprint area of the delamination damage can be calculated by using an ImageJ algorithm.

A photograph of a typical indentation caused by the striking of the impactor on the CFRP panel is shown in Figure 2. The depth of this indentation was measured employing two very different methods. Firstly, a handheld digital depth gauge was used to measure the indentation depth immediately after impact, and then 24 hours and 48 hours after the impact event. The depth reduction over time due to relaxation of the composite was minimal, i.e. no more than 20  $\mu\text{m}$ , and after 48 hours a steady-state, permanent indentation was recorded. These are the depth values presented below. For each measurement value, the indentation measurement was repeated eight times. Each time the gauge was rotated by 45° in order to account for any surface defect which could have raised the gauge and led to an inaccurate depth reading. An average was taken to give the measurement value. Secondly, an Olympus Lext OLS5000 Confocal Laser Scanning Microscope was also used to give a 3D surface scan, 12 mm x 12 mm in size, of each panel, from which an accurate value of the surface indentation could be identified, after removing any effects from any tilting of the panel. As shown in Figure 3, the results from the Confocal microscope align closely with those from the handheld depth gauge, justifying that the handheld gauge could give accurate indentation depth readings in a quick, easy and cheap manner.

Finally, specimens were cut, using a diamond blade, from the centre of a panel, on a line parallel to the 100 mm edges of the panel. The edges of these specimens were then ground and polished, using silicon carbide grinding paper and diamond suspension fluid on a polishing cloth, respectively. They were then viewed using a Zeiss Axio Scope A1 optical microscope.

### **3. Results and discussion**

#### **3.1. Delamination, i.e. interlaminar, damage**

Figures 4 and 5 show the C-scan damage maps for two repeat tests after impacts at 2, 5, 10, 15 and 20 J for the two thicknesses, i.e. 2.3 and 4.6 mm, of CF/Epoxy panels, with the corresponding scales showing the depth of each delamination beneath the impacted surface. Note that 20 J impact tests were not performed on the 2.3 mm thick CF/Epoxy panels since the damage severity would have been too great, potentially causing damage to the drop-weight tower. In such figures, as noted above, the damage area (DA) is indicated and was calculated by counting the number of pixels that were not dark blue in colour, since dark blue corresponds to areas of the laminate free from delaminations. The results from the replicate tests demonstrate the high level of reproducibility achieved in the present study. As expected, the extent of delamination increases as the impact energy is increased. The delaminations propagate at ply boundaries where the fibre direction in adjacent plies differs [14,15], i.e. not

between blocked plies. This is because the dramatic change in stiffness in a particular direction from one ply to the next at the ply boundaries generates high interfacial stresses, leading to delamination [16]. The direction of delamination propagation is usually dictated by the orientation of the ply directly beneath the delamination [15]. This explains the direction of the characteristic peanut-shaped delamination footprints.

Figure 6 compares the C-scan damage maps obtained in the 2.3 mm and 4.6 mm material at a given impact energy. Note that just the first scan is shown for each thickness and was arbitrarily chosen. The difference in the delamination damage area for the 2.3 mm and 4.6 mm panels can be clearly seen. For the same impact energy, the 4.6 mm specimens exhibit a greater delamination area than the 2.3 mm specimens. The difference in delamination area increases with increasing impact energy. This can be explained as intralaminar cracks and delaminations tend to form a conical shape through the thickness of the material, with wider delaminations at the base [17]. Hence, in a thicker panel a greater area of delamination damage is formed in the rear of the specimen, leading to a larger total damage area. The CFRP test panels impacted at 2 J show very little delamination damage in the case of the 2.3 mm thickness panel and in the case of the 4.6 mm specimens no delamination damage at all is detected. This suggests that the threshold energy for damage to occur for the 2.3 mm thick test panels is just below 2 J and the threshold energy for the 4.6 mm thick specimens is between 2 and 5 J. The delaminations visible in the 2.3 mm thickness specimens are close to the rear surface. This observation suggests that, at very low impact energies, the impactor may not be able to initiate matrix cracks in the front face. However, instead, for the 2.3 mm thick panels, delamination occurs near the rear surface due to bending and the resulting higher tensile and shear stresses across the ply interfaces near the rear impacted surface. For the 4.6 mm thick specimens, at an impact energy of 2 J, the bending deformation would be less marked and hence delaminations at the rear ply interfaces do not occur.

### **3.2. Load versus time and load versus displacement results**

Load versus time and load versus displacement traces are shown in Figure 7 for impacts at 2, 5, 10, 15 and 20 J on both thicknesses of CFRP. The small sinusoidal oscillations on the rising section of the traces are indicative of mass-spring oscillations and have been observed by other researchers [18-20]. Clear load drops, which are seen for most of the composite panels, show the load and time at which damage initiated in the specimens during the impact event. The load versus time traces, shown in Figure 7a, for the 2 and 5 J impact energy cases for the 2.3 mm thickness panels, do not show a clear load drop, despite damage clearly having occurred, as shown by subsequent C-scans, see Figure 6. In this figure there may be seen to be some very slight delamination damage observed at the 2 J impact for the thin specimen of

2.3 mm thickness near the rear surface of the specimen but no damage was observed for the 2 J impact for the thicker specimen of 4.6 mm in thickness. Thus, at these relatively low impact energies, and for the more flexible 2.3 mm thick specimen, the load drop which is indicative of the damage threshold is less noticeable in Figure 7a. The results shown in Figure 7b for the load versus displacement traces clearly demonstrate the different stiffnesses of the two thicknesses of CFRP panel.

Some impact events were also recorded using two high-speed cameras. Figure 8 shows a sequence of high-speed images which clearly illustrate the indentation process for an impact of 15 J on a 4.6 mm thick CFRP composite panel, with an inter-frame time of 1 ms. The first image (frame 1 - top left) is captured just before the impact event and the total contact time is approximately 5 ms, with the last image (frame 6 - bottom right) showing the start of the rebounding of the impactor. Figure 8 clearly shows that the impactor indents the front surface and that there is a clear contact area for frames 2, 3, 4 and 5. The deformation beneath the impactor exhibits both viscoelastic and plastic behaviour. This indentation damage is also accompanied by intralaminar damage, involving matrix cracking within the ply and fibre debonding and fracture and, in addition, delamination between the differently orientated plies, see Figure 6 and as discussed below. After the impact event, a residual permanent indentation, see Figure 2, is left in the panel from this plasticity, intralaminar and interlaminar damage.

Energy versus time graphs are shown in Figure 9 for all the impact energies for tests on both thicknesses of CFRP composite panel. These show that the rebound energy increases for relatively high impact energies for both thicknesses. At low impact energies, the panel is more able to absorb the energy of the impact event locally with less rebound energy provided back to the impactor. As the impact energy increases, the whole test panel deforms and acts like a spring, storing elastic strain-energy which is then available to rebound the impactor. Of course, some of this energy is lost in intralaminar damage around the impactor, delamination between the plies and friction, vibration and acoustic losses, particularly around the supports.

### **3.3. Indentation depth studies**

Figure 10 shows cross-sections of the resulting indentations after 2, 5, 10, 15 and 20 J impact energies for each thickness of CF/Epoxy composite, taken from the Confocal microscopy measurements. An impact at 20 J was not performed on the 2.3 mm material, as discussed above. From these cross-sections, an indentation depth was calculated and compared with the indentation depth measurements taken from using the handheld digital gauge and, as shown previously in Figure 3, the two different methods of measuring the indentation depth are in excellent agreement. These results, given in Figure 10, generally show that a section



through the permanent indentation profile has a central depression, with gently shelving sides, and this shape deepens with impact energy.

Figure 11 presents the indentation depths measured for different impact energies, and also the associated delamination damage areas versus the impact energy, for both the 2.3 mm thick (Figure 11(a)) and the 4.6 mm thick (Figure 11(b)) panels. In most cases, a third replicate result, in addition to the duplicate results presented in Figures 4 and 5, is also included to improve the confidence in these data. As may be seen, the data points for the plots of damage area versus impact energy for both the 2.3 and 4.6 mm thick panels lie on an approximately linear relationship, whilst those for the plots of indentation depth versus impact energy do not. This aspect is discussed in detail below.

The results for the indentation depth versus the impact energy, and versus the associated damage area, for the two different thicknesses of panel, are compared in Figure 12. It is shown in Figure 12(a) that there is little effect of the thickness of the panel on the indentation depth incurred from the impact event. Thus, for an impact event at the same impact energy, the CF/Epoxy composite panels of a thickness of 4.6 mm show a similar indentation depth to the panels of a thickness of 2.3 mm. This observation is in contrast to that from the work of Shuck, as cited by Talreja and Phan [6], and of Panettieri [11]. These authors found that thinner CFRP composites showed a larger indentation depth.

On the other hand, the relationship between the indentation depth and the damage area, for a given impact energy, as shown in Figure 12(b), reveals a very significant effect of the panel thickness, with the thicker 4.6 mm panel suffering more damage for a given indentation depth when the impact energy is greater than about 5 J. This arises, of course, from the results shown in Figures 6, 10 and 11. Thus, whilst the indentation depths are similar in value for a given impact energy in the two panels, see Figure 12(a), the corresponding damage areas are significantly greater for the 4.6 mm panel at an impact energy of about 5 J and above, see Figure 12(b). Interestingly, for both thicknesses of panel, Figure 12(b) reveals that an indentation may occur in a panel with little, or no, accompanying damage area. For example, at an impact energy of 2 J both panel thicknesses exhibit a clearly visible indentation after the impact event, see Figures 10 and 12(b), whilst the associated damage area for the 2.3 mm panel is very localised at about 8 mm<sup>2</sup> and there is no damage area observed at all for the 4.6 mm panel. These observations strongly suggest that the indentation damage is initiated before any delamination damage develops.

Finally, Figure 13 shows that all the relationships between the indentation depth and the damage area for both thicknesses of panel from Figure 12(b) can be unified to give a 'master' relationship, which is not linear, by plotting the indentation depth versus the

associated damage area normalised with respect to the panel thickness. By normalising the damage area by dividing by the panel thickness, almost all the resulting data points for impact energies of 2, 5, 10 and 15 J converge onto an approximately unique ‘master’ line, as shown in Figure 13. Several interesting points arise from Figure 13. Firstly, from the impact tests on both composite panels, of thickness 2.3 mm and the 4.6 mm, at impact energies above about 15 J it appears that the increase in indentation depth does not keep rising at the same rate as that of the damage area as a function of the impact energy. Secondly, the unique relationship in Figure 13 demonstrates that there is no need to have separate relationships for each thickness of composite when comparing the measured indentation depth against the corresponding delamination damage area. Thirdly, by assuming this unique ‘master’ relationship is indeed valid for all appropriate thicknesses of this lay-up within a range of at least 2.3 to 4.6 mm based on the current tests, one can (a) measure the indentation depth, (b) then read off the corresponding normalised damage area, and (c) then, from a knowledge of the chosen composite’s thickness, the approximate damage area can be calculated. Fourthly, it may be noted that to take into account varying lay-ups of the same composite material, and hence differing numbers of interfaces where delamination can occur, normalisation by the bending stiffness could be used. For example, in the present study, for the 4.6 mm thickness laminate, the blocking of two plies for each fibre orientation was employed to reduce the number of interfaces where delamination occurs, so that the delaminations are more clearly visible with the ultrasonic C-scan technique. It should be pointed out that a  $[45/-45/0/90]_{2s}$  layup could be used which would have the same thickness, i.e. 4.6 mm, but double the number of ply interfaces, i.e. twelve rather than six, and all these interfaces could be potential locations for delamination initiation. However, given that alternative lay-ups were not tested in the present study, the simpler normalisation method based only on the thickness was used.

With the results above in mind, a possible explanation of why the indentation depth is related to the delamination area as shown in Figures 12(b) and 13 may follow from earlier research by Tabor [3]. He suggested that, as the initial impact energy for the impactor is increased, there is indeed a relationship between the resulting depth of indentation,  $d$ , and the initial impact energy of the impactor,  $U_{impactor}$ , but only once the impact energy for yielding of the material, and hence the associated permanent indentation,  $U_{yield}$ , has been exceeded. He assumed a linear relationship but in the analysis below, to provide a more general representation of the experimental data, a second-order polynomial relationship is employed. Thus, we have:

$$d = k_{1\text{ indentation}} \cdot (U_{impactor} - U_{yield}) + k_{2\text{ indentation}} \cdot (U_{impactor} - U_{yield})^2 \quad (1)$$

with the threshold condition:

$$d = 0 \quad \text{for } U_{impactor} < U_{yield}$$

Where  $k_{1\text{ indentation}}$  and  $k_{2\text{ indentation}}$  are first-order and second-order parameters for the second-order polynomial fit. Now, from research by Liu et al. [21], an approximately linear relationship exists between the footprint area,  $A$ , of the delamination damage and the impact energy,  $U_{impactor}$ , once the threshold energy for delamination,  $U_{threshold}$ , which is related to the threshold load, is exceeded. This observation is in agreement with the results shown in Figure 11 (see lower graphs). Thus:

$$A = k_{delamination} \cdot (U_{impactor} - U_{threshold}) \quad (2)$$

with the threshold condition:

$$A = 0 \quad \text{for } U_{impactor} < U_{threshold}$$

and where  $k_{delamination}$  is a constant of proportionality.

These equations are fitted to the data points given in Figure 11 and 12 using the constants given in Table 1. As may be seen, these simple relationships are in good agreement with the experimentally measured results.

Combining Equations (1) and (2) to eliminate the initial impact energy, it can be shown that the indentation depth versus delamination footprint area will also be a second-order polynomial of the form:

$$d = \left( \frac{k_{1\text{ indentation}}}{k_{delamination}} \right) \cdot (A + C') + \left( \frac{k_{2\text{ indentation}}}{k_{delamination}^2} \right) \cdot (A + C')^2 \quad (3)$$

which can be expanded to give:

$$d = \left( \frac{k_{1\text{ indentation}}}{k_{delamination}} \right) \cdot A + \left( \frac{k_{2\text{ indentation}}}{k_{delamination}^2} \right) \cdot A^2 + \left( \frac{2k_{2\text{ indentation}}}{k_{delamination}^2} \right) \cdot A \cdot C' + \left( \frac{k_{2\text{ indentation}}}{k_{delamination}^2} \right) \cdot C'^2 + \left( \frac{k_{1\text{ indentation}}}{k_{delamination}} \right) \cdot C' \quad (4)$$

Here the constant  $C'$  ( $C' = k_{delamination} \cdot (U_{threshold} - U_{yield})$ ) is a positive quantity since yielding, which gives rise to the indentation, has been found to occur at a slightly lower impact energy than the threshold impact energy for delamination, as noted above. Indeed, it is suggested that, at least in the present tests, indentation is a prerequisite for delamination damage. (Since, the indentation process provides for shear and tensile loading of the ply interface and so indentation occurs at a lower impact energy than for delamination.) Therefore, a second-order polynomial relationship between indentation depth,  $d$ , and delamination footprint area,  $A$ , is to be expected, with a positive intercept on the vertical indentation depth axis, as is indeed

apparent in Figure 13. The positive intercept, on the vertical axis of indentation depth versus delamination footprint area curve, is given by the term:

$$\left(\frac{k_2 \text{ indentation}}{k_{delamination}^2}\right) \cdot C'^2 + \left(\frac{k_1 \text{ indentation}}{k_{delamination}}\right) \cdot C' \quad (5)$$

which is greater than zero, if  $C' > 0$  (or  $U_{threshold} > U_{yield}$ ) as is usually the case, with the indentation damage occurring at a slightly lower impact energy than the delamination damage. As may be seen from Figure 13, the experimental results are in good agreement with the fit provide by the above equations, using the values of the various parameters in these equations as given in Table 1.

It is expected that similar relationships to those identified in the present study between indentation depth and delamination damage area would be obtained for other composite laminates, for both thermoset and thermoplastic matrices. Similar relationships may also be obtained for other types of continuous-fibre composites, e.g. woven fibre composites. However, in order to use this method for a given composite material, a unique 'master' curve of indentation depth versus normalised damage area must firstly be established through impact testing for the specific composite of interest.

### 3.4. Optical microscopy studies

Firstly, it should be noted that the full delamination lengths seen in the optical microscope images were similar in value to the delamination lengths detected by the ultrasonic C-scans. However, the full delamination lengths are not shown for the optical microscope images in order to show the intralaminar cracking in detail.

Figure 14 shows a central cross-section, cut directly beneath the indentation along a line parallel to the 100 mm edge, from a 4.6 mm thick composite panel that had been subjected to a 15 J impact. The various types of microstructural damage sustained during the impact are highlighted. The intralaminar damage mainly consists of matrix cracks which are initiated at the impact site and then radiate outwards. These cracks propagate through the plies of the composite until they reach an interlaminar delamination, which occurs where adjacent plies have differing orientations. At this point, the intralaminar cracks can initiate a further delamination which propagates in a direction away from the impact site. This interlaminar delamination damage is the type of damage that is detected in the ultrasonic C-scans. Fibre debonding and fracture are other forms of intralaminar damage which take place and these are visible in Figure 14 as a kink band. Fracturing the fibres can significantly reduce the residual stiffness of the composite. Finally, the resulting indentation is clearly visible on the top surface of the panel in the lower micrograph in Figure 14.

Figure 15 compares cross-sections of composite panels of thicknesses of 2.3 mm and 4.6 mm, both having been impacted at 15 J. These two micrographs highlight the conical-shaped intralaminar cracking zone which occurs through the thickness of the composite panel during the impact event. Thus, leading to the increased delamination area in the 4.6 mm composite panels compared to the 2.3 mm panels. It is interesting that, although more delamination damage is seen in the 4.6 mm panel, a greater severity of intralaminar damage is seen in the 2.3 mm panel as the deflection of the panel is greater during the impact event, see Figure 7b.

#### **4. Conclusions**

The present study has shown that:

- For composite panels of 4.6 mm in thickness there is generally a larger delamination damage area observed than for a panel of 2.3 mm in thickness, when impacted at the same impact energy. This is due to the delamination and intralaminar damage spreading out like a cone from the impact site. It is suggested that the matrix cracking and other types of intralaminar damage in the ply are strongly linked to the shear and tensile loading of the ply interface beneath the ply, leading to interlaminar, i.e. delamination, damage occurring at this lower ply interface. For these reasons, with a thicker panel the extent of the delamination increases away from the impacted face, with a larger extent of the delaminations near the rear face.
- The deformation that results from any indentation in the surface of the composite panel caused by the impactor exhibits both viscoelastic and plastic behaviour. The reduction in the depth of the indentation that occurs over time due to relaxation of the composite is minimal, i.e. no more than 20  $\mu\text{m}$ , and after 48 hours a steady-state permanent indentation is recorded. These are the depth values used in the present paper for subsequent analysis.
- This indentation damage is also accompanied by intralaminar damage, involving matrix cracking within the ply and fibre debonding and fracture, and interlaminar damage, i.e. delaminations, between the differently orientated plies.
- The indentation depth has been shown to be related to the delamination damage area for the low-velocity impact energies of 2 to 20 J by a second-order polynomial relationship. This arises because the indentation depth has a second-order polynomial relationship with the impact energy but the delamination footprint area has a linear relationship with the impact energy. The indentation occurs in the impact test at a slightly lower impact energy than that required for interlaminar delamination damage to initiate and develop. At higher impact energies there is a saturation effect where it

becomes more difficult for the indentation to increase in depth and hence the nonlinear second-order relationship is observed. These observations strongly suggest that the indentation damage is initiated before any delamination damage develops.

- For the 2.3 and 4.6 mm thick composite panels, there is a unique ‘master’ relationship between the indentation depth and the normalised interlaminar delamination damage area, i.e. the damage area divided by the panel thickness, for impact energies up to 15 J.
- Measuring the indentation depth has the potential to be used as a quick and cheap alternative to employing expensive ultrasonic C-scan or X-ray Computed Tomography equipment for estimating the extent of internal interlaminar delamination damage.

### Acknowledgements

This paper has been put together for the Special Memorial Issue of Applied Composite Materials (ACMa), dedicated to the Founding Editor of the ACPMa journal, Professor Peter Beaumont. The Authors very much appreciate the many interactions and thoughtful discussions, over the years, with Professor Peter Beaumont of the University of Cambridge. The authors would like to express their appreciation to Dr. Ruth Brooker and Mr. Suresh Viswanathan-Chettiar at Imperial College London for their valuable support on the experimental testing conducted in the present research. For the purpose of open access, the authors have applied a Creative Commons Attribution (CC BY) license to any Author Accepted Manuscript version arising.

**Competing interests.** The authors declare that they have no competing interests.

### References

- [1] Vaidya U. Impact Response of Laminated and Sandwich Composites. In: Abrate S (ed.) *Impact Engineering of Composite Structures*. Vienna: Springer; 2011. p. 97-191.
- [2] Cantwell W, Morton J. Comparison of the low and high velocity impact response of CFRP. *Composites*. 1989;20(6):545-551. Available from: [https://doi.org/10.1016/0010-4361\(89\)90913-0](https://doi.org/10.1016/0010-4361(89)90913-0)
- [3] Hutchings IM. The contributions of David Tabor to the science of indentation hardness. *Journal of Materials Research*. 2009;24(3):581-589. Available from: <https://doi.org/10.1557/jmr.2009.0085>
- [4] Wardle BL, Lagace PA. On the use of dent depth as an impact damage metric for thin composite structures. *Journal of Reinforced Plastics and Composites*. 1997;16(12): 1093-1110. Available from: <https://doi.org/10.1177/073168449701601202>

- [5] Shi Y, Swait T, Soutis C. Modelling damage evolution in composite laminates subjected to low velocity impact. *Comp Struct.* 2012;94(9):2902-2913. Available from: <https://doi.org/10.1016/j.compstruct.2012.03.039>
- [6] Wagih A, Maimi P, Blanco N, Costa J. A quasi-static indentation test to elucidate the sequence of damage events in low velocity impacts on composite laminates. *Comp. Part A.* 2016;82:180-189. Available from: <https://doi.org/10.1016/j.compositesa.2015.11.041>
- [7] Komorowski JP, Simpson DL, Gould RW. A technique for rapid impact damage detection with implication for composite aircraft structures. *Composites.* 1990;21(2):169-173. Available from: [https://doi.org/10.1016/0010-4361\(90\)90009-L](https://doi.org/10.1016/0010-4361(90)90009-L)
- [8] Talreja R, Phan N. Assessment of damage tolerance approaches for composite aircraft with focus on barely visible impact damage. *Comp Struct.* 2019;219:1-7. Available from: <https://doi.org/10.1016/j.compstruct.2019.03.052>
- [9] Vieille B, Casado VM, Bouvet C. Influence of matrix toughness and ductility on the compression-after-impact behavior of woven-ply thermoplastic- and thermosetting-composites: A comparative study. *Comp Struct.* 2014;110:207-218. Available from: <https://doi.org/10.1016/j.compstruct.2013.12.008>
- [10] Leicy D, Hogg PJ. The effect of crystallinity on the impact properties of advanced thermoplastic composites. In: Bunsell AR et al. (eds.) *Developments in the Science and Technology of Composite Materials.* Dordrecht: Springer; 1989. p. 809-815.
- [11] Panettieri E, Fanteria D, Montemurro M, Froustey C. Low-velocity impact tests on carbon/epoxy composite laminates: A benchmark study. *Comp Part B.* 2016;107:9-21. Available from: <http://dx.doi.org/10.1016/j.compositesb.2016.09.057>
- [12] Bouvet C, Rivallant S, Barrau JJ. Low velocity impact modeling in composite laminates capturing permanent indentation. *Comp Science and Tech.* 2012;72(16):1977-1988. Available from: <http://dx.doi.org/10.1016/j.compscitech.2012.08.019>
- [13] ASTM International. Standard Test Method for Measuring the Damage Resistance of a Fiber-Reinforced Polymer Matrix Composite to a Drop-Weight Impact Event (D7136/D7136M-15). Annual Book of ASTM Standards West Conshohocken, PA, USA; 2015.
- [14] Liu H, Liu J, Ding Y, Zheng J, Kong X, Zhou J, Harper L, Blackman BRK, Kinloch AJ, Dear JP. The behaviour of thermoplastic and thermoset carbon fibre composites subjected to low-velocity and high-velocity impact. *Journal of Materials Science.* 2020;55:15741-15768. Available from: <https://doi.org/10.1007/s10853-020-05133-0>
- [15] Liu H, Falzon BG, Tan W. Experimental and numerical studies on the impact response of damage-tolerant hybrid unidirectional/woven carbon-fibre reinforced composite laminates. *Comp Part B.* 2018;136:101-118. Available from: <https://doi.org/10.1016/j.compositesb.2017.10.016>
- [16] Wisnom M. The role of delamination in failure of fibre-reinforced composites. *Phil. Trans. A.* 2012;370(1965):1850-1870. Available from: <https://doi.org/10.1098/rsta.2011.0441>
- [17] Cantwell W, Morton J. Impact perforation of carbon fibre reinforced plastic. *Comp Science and Tech.* 1990;38(2):119-141. Available from: [https://doi.org/10.1016/0266-3538\(90\)90002-M](https://doi.org/10.1016/0266-3538(90)90002-M)
- [18] Dear JP, MacGillivray JH. Strain gauging for accurate determination of K and G in impact tests. *Journal of Materials Science.* 1991;26:2124-2132. Available from: <https://doi.org/10.1007/BF00549178>
- [19] Williams JG, Adams GC. The analysis of instrumented impact tests using a mass-spring model. *Int Journal of Fracture.* 1987;33:209-222. Available from: <https://doi.org/10.1007/BF00013171>

- [20] Dear JP. High-speed photography of impact effects in three-point bend testing of polymers. *Journal of Applied Physics*. 1990;67(9):4304-4312. Available from: <https://doi.org/10.1063/1.344946>
- [21] Liu H, Liu J, Ding Y, Hall ZE, Kong X, Zhou J, Blackman BRK, Kinloch AJ, Dear JP. A three-dimensional elastic-plastic damage model for predicting the impact behaviour of fibre-reinforced polymer-matrix composites. *Comp Part B*. 2020;201:108389. Available from: <https://doi.org/10.1016/j.compositesb.2020.108389>



Table 1. The values of the constants in Equations (1) and (2) and the approximate initiation energies required for indentation and delamination.

	<b>2.3 mm</b>	<b>4.6 mm</b>
$k_1$ indentation (mm/J)	0.0209	0.0251
$k_2$ indentation (mm/J)	-0.0004	-0.0006
$k_{\text{delamination}}$ (mm <sup>2</sup> /J)	47.8	144.5
$U_{\text{yield}}$ (J)	~0.5	~1.4
$U_{\text{threshold}}$ (J)	~1.3	~3.1

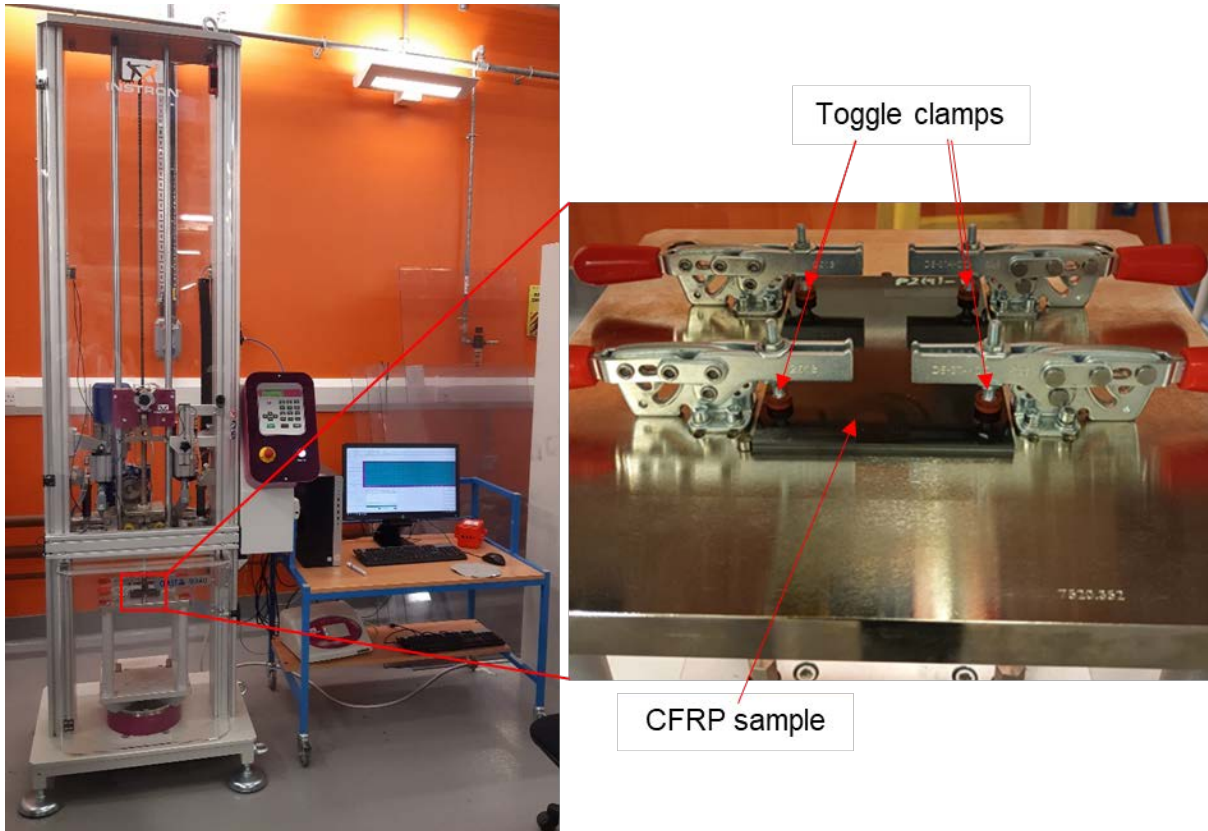


Figure 1. The experimental impact drop-weight equipment.



Figure 2. Photograph of a CF/Epoxy composite panel 150 mm x 100 mm in size with a thickness of 4.6 mm after an impact of 7.5 J showing a typical surface indentation.

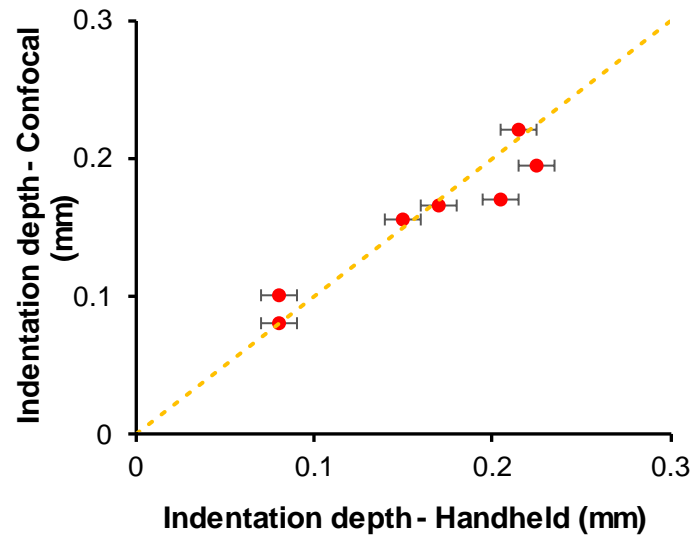


Figure 3. The indentation depth in the CF/Epoxy composite panel measured using the Confocal laser scanning microscope versus using the handheld gauge.

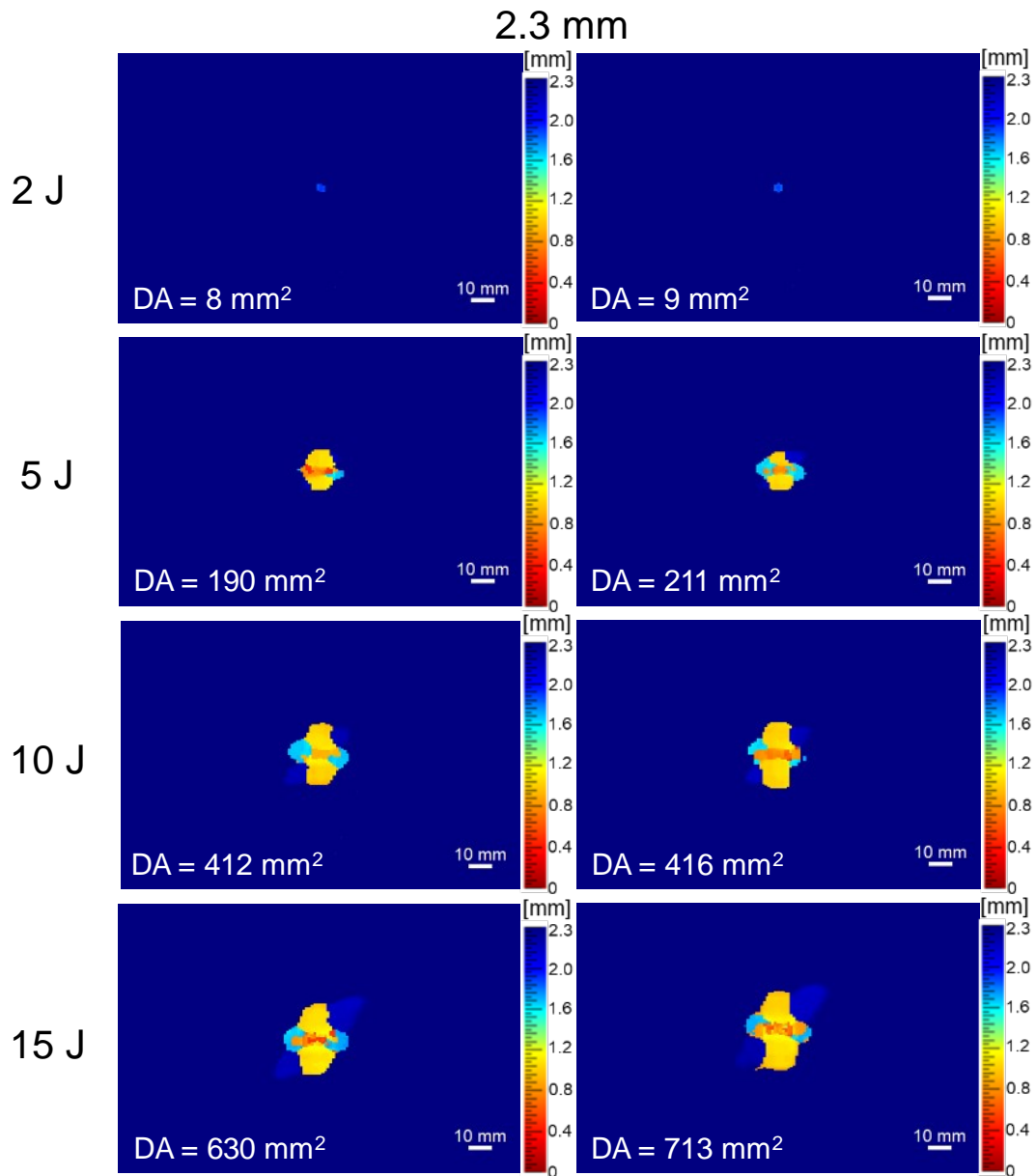


Figure 4. C-scan damage maps obtained from the CF/Epoxy replicate composite panels with a thickness of 2.3 mm with impact energies of 2 J, 5 J, 10 J and 15 J. The right-hand side scale indicates the location of the interlaminar delamination as a function of the depth through the thickness of the panel (0 to 2.3 mm), where the dark red colour represents the front (impacted) face and the dark blue colour represents the rear (non-impacted) face of the composite panel. The footprint of the delamination damage area (DA) detected is given in the bottom left-hand corner for each specimen and was determined by counting the pixels which had a colour which was not dark blue. The bottom right of each damage map shows a 10 mm scale bar.

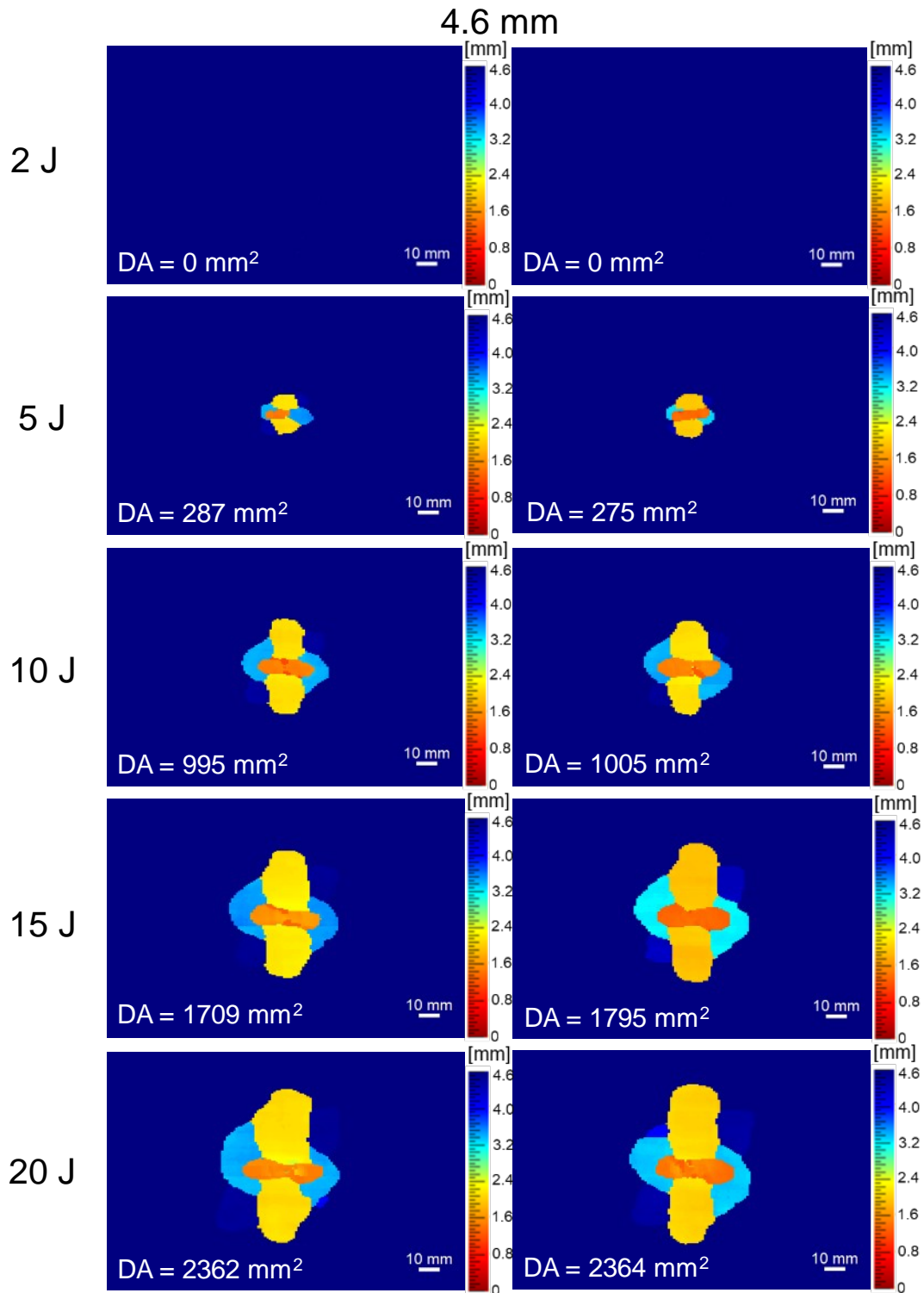


Figure 5. C-scan damage maps obtained from the CF/Epoxy replicate composite panels with a thickness of 4.6 mm with impact energies of 2 J, 5 J, 10 J, 15 J and 20 J. The right-hand side scale indicates the location of the interlaminar delamination as a function of the depth through the thickness of the panel (0 to 4.6 mm), where the dark red colour represents the front (impacted) face and the dark blue colour represents the rear (non-impacted) face of the composite panel. The footprint of the delamination damage area (DA) detected is given in the bottom left-hand corner for each specimen and was determined by counting the pixels

which had a colour which was not dark blue. The bottom right of each damage map shows a 10 mm scale bar.

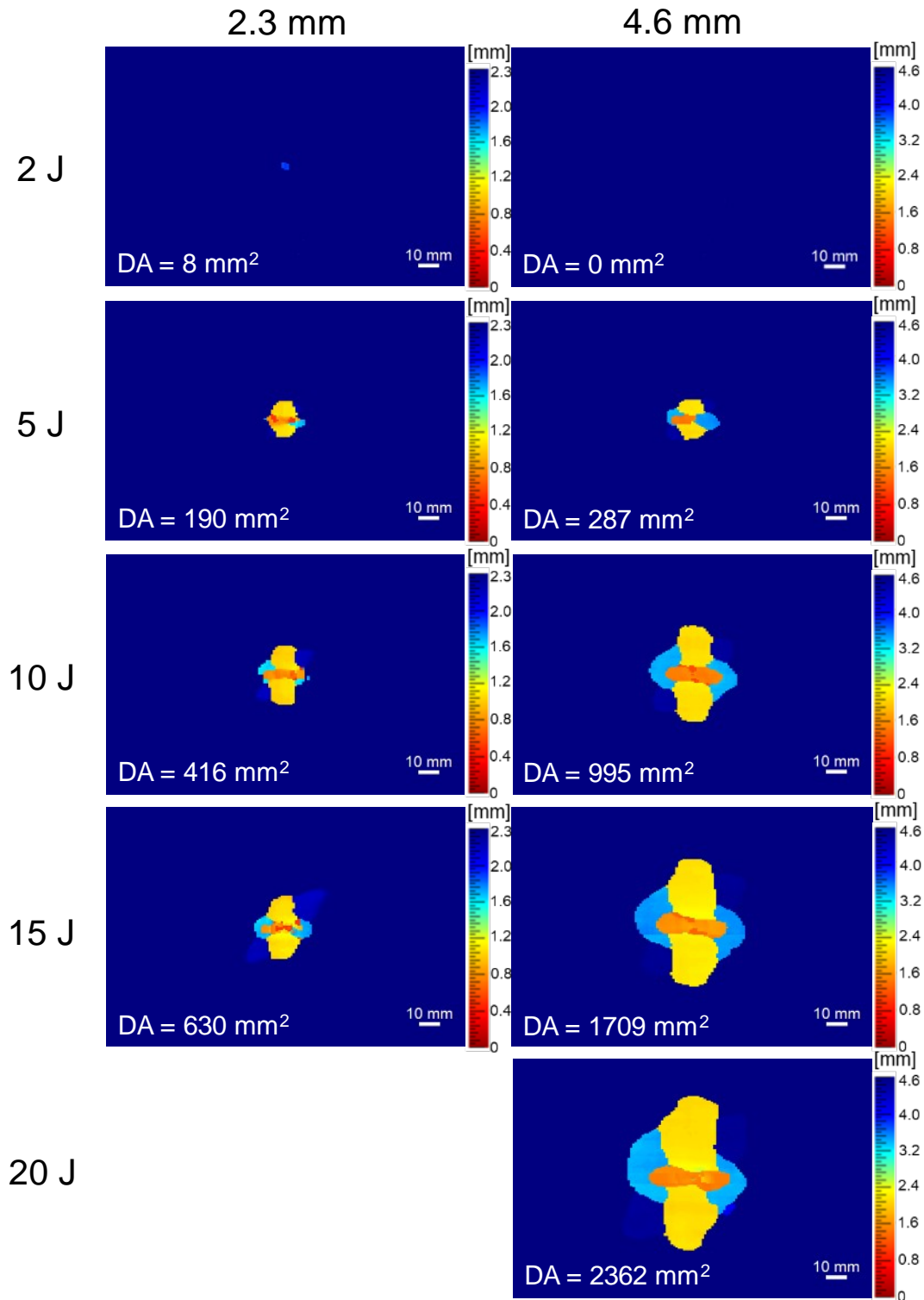


Figure 6. Comparison of the C-scan damage maps obtained from the impacted CF/Epoxy composite panels with a thickness of 2.3 or 4.6 mm. The right-hand side scale indicates the location of the interlaminar delamination as a function of the depth through the thickness of the panel, where the dark red colour represents the front (impacted) face and the dark blue colour represents the rear (non-impacted) face of the composite panel. The footprint of the delamination damage area (DA) detected is given in the bottom left-hand corner for each specimen and was determined by counting the pixels which had a colour which was not dark blue. The bottom right of each damage map shows a 10 mm scale bar.

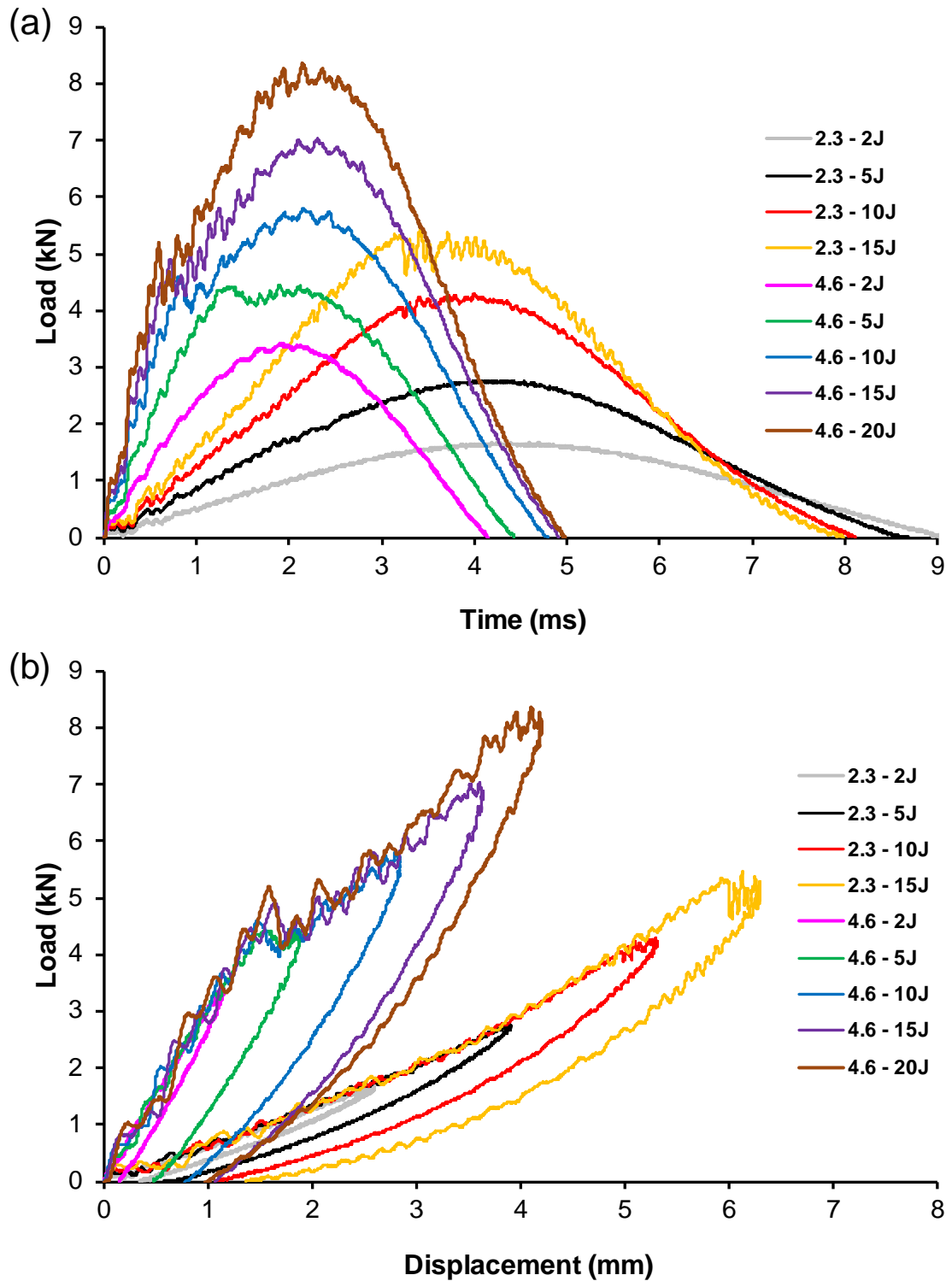


Figure 7. (a) Load versus time traces and (b) load versus displacement traces for 2.3 mm and 4.6 mm thick CF/Epoxy composite panels impacted at 2 J, 5 J, 10 J, 15 J and 20 J.



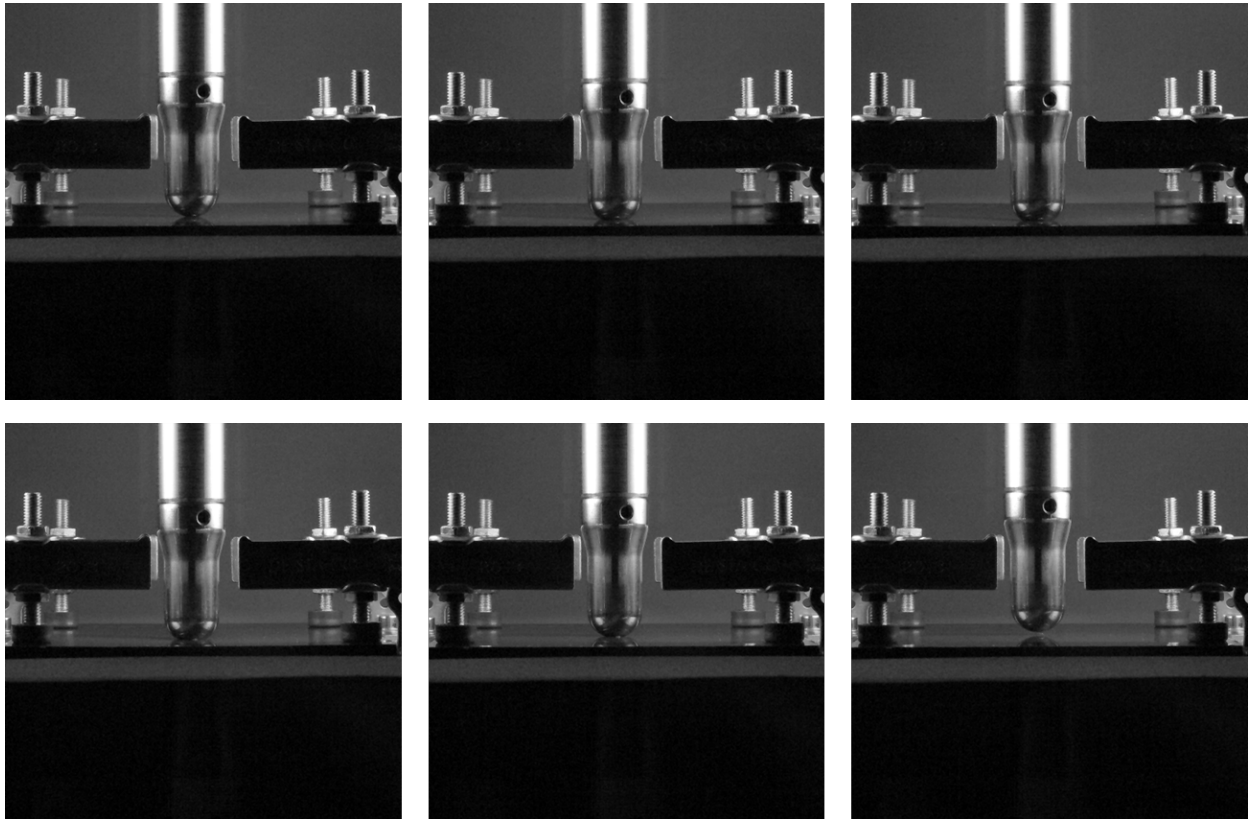


Figure 8. Series of high-speed photographic images showing the indentation process for an impact of 15 J on a 4.6 mm thick CF/Epoxy composite panel (inter-frame time is 1 ms). The first image (top left) is captured just before the impact event and the total contact time is approximately 5 ms, with the last image (bottom right) showing the start of the rebounding of the impactor. The hemispherical stainless-steel impactor has a diameter of 16 mm.

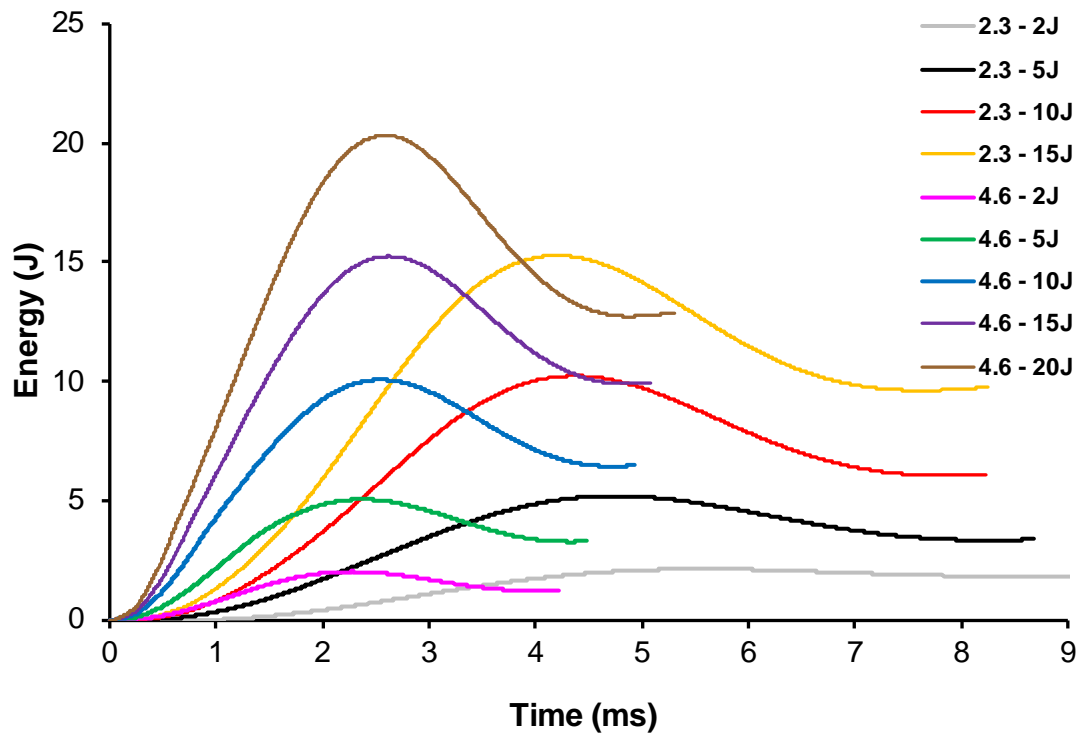


Figure 9. Energy versus time traces for 2.3 mm and 4.6 mm thick CF/Epoxy composite panels for impact energies of 2 J, 5 J, 10 J, 15 J and 20 J.

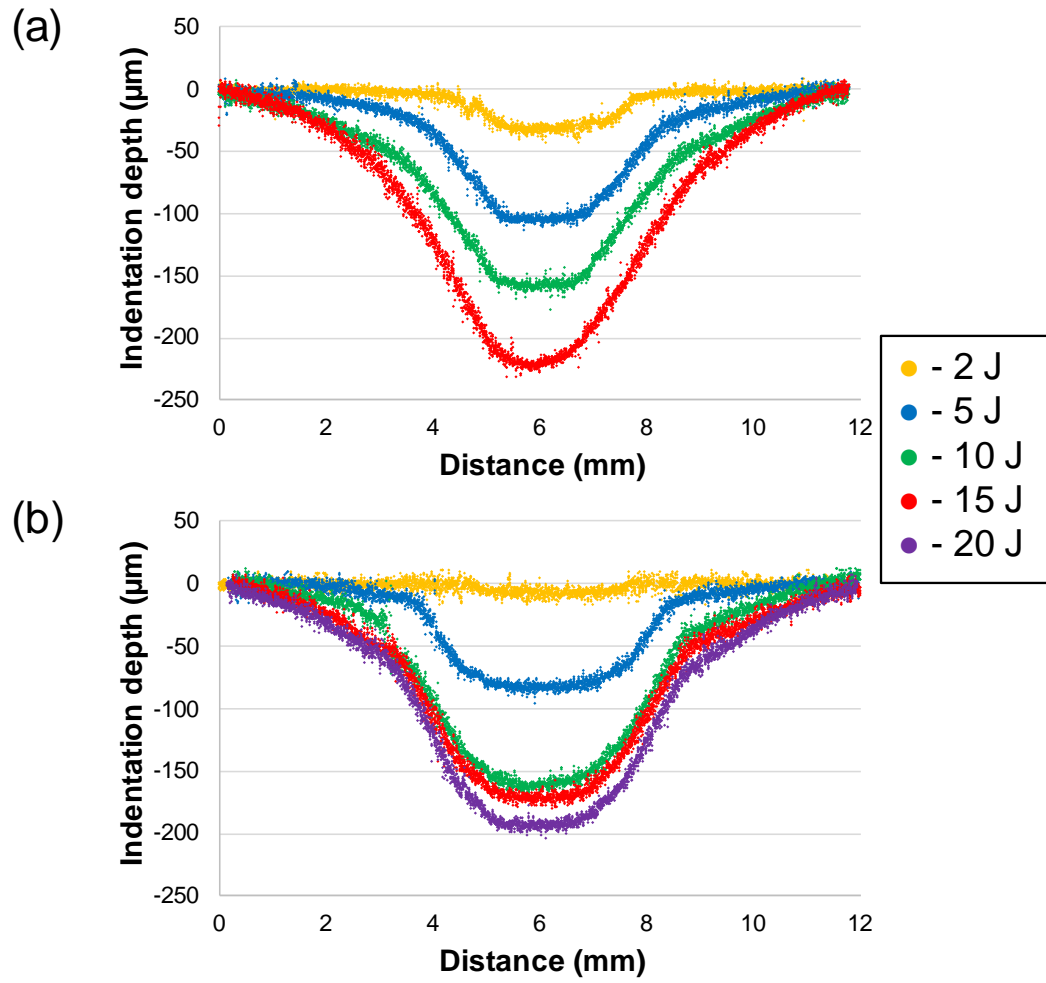


Figure 10. Typical indentation cross-section in (a) 2.3 mm thick and (b) 4.6 mm thick CF/Epoxy composite panels after an impact of 2 J, 5 J, 10 J, 15 J and 20 J.

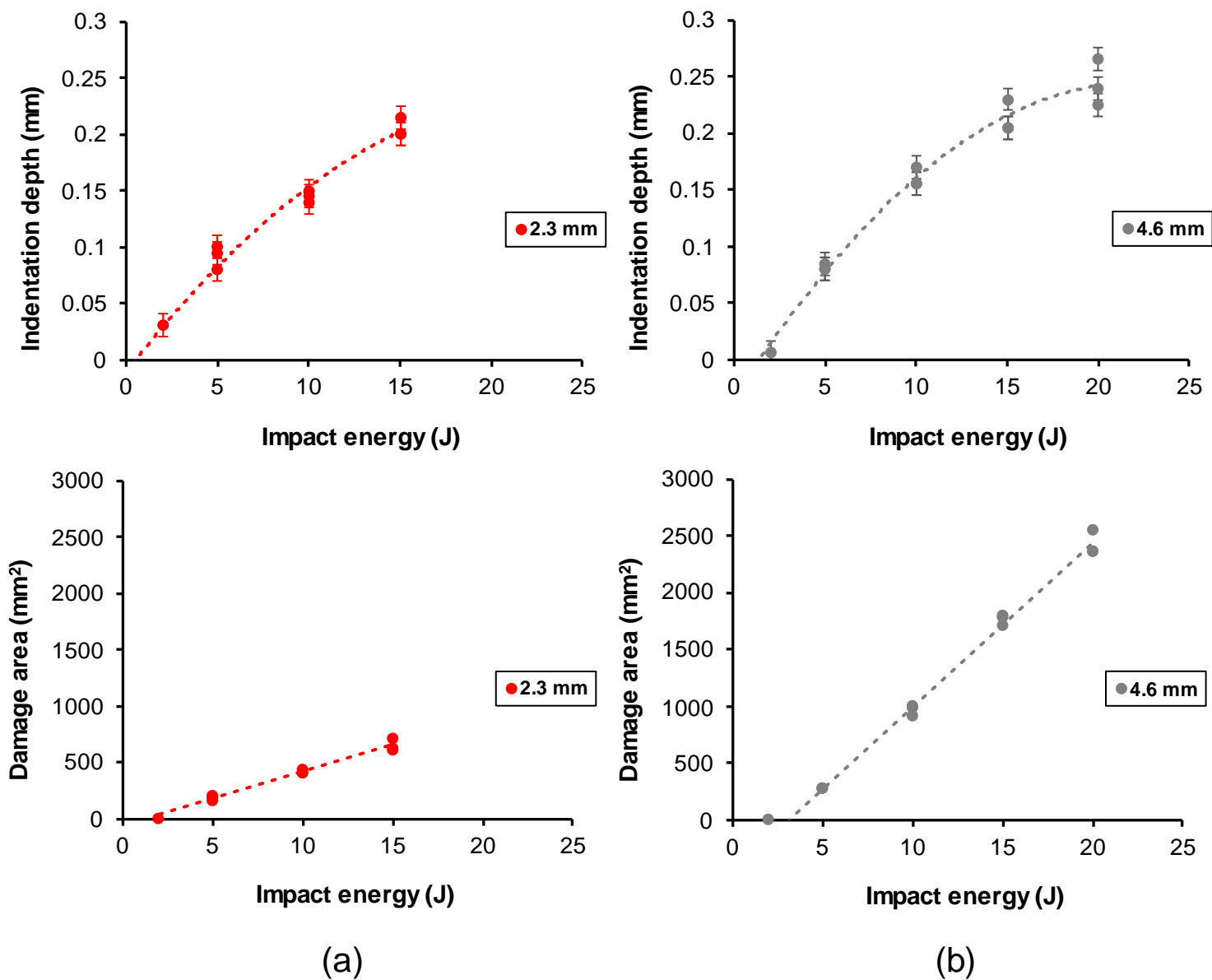


Figure 11. The indentation depth versus impact energy, and delamination damage area versus impact energy, for the CF/Epoxy composite panels of (a) thickness 2.3 mm and (b) thickness 4.6 mm, for the two replicate cases presented in Figures 4 and 5 and, in some cases, for a third replicate test.

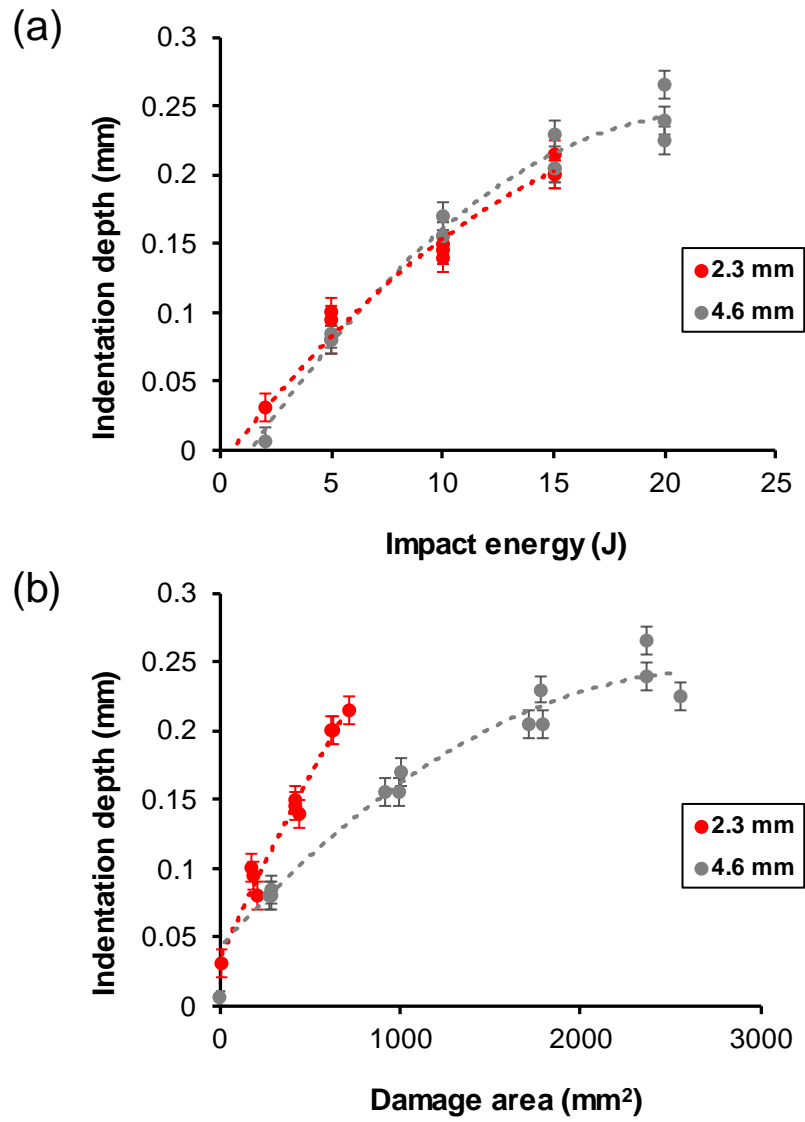


Figure 12. The indentation depth versus (a) the impact energy and (b) the interlaminar damage area for the 2.3 mm and 4.6 mm thick CF/Epoxy composite panels.

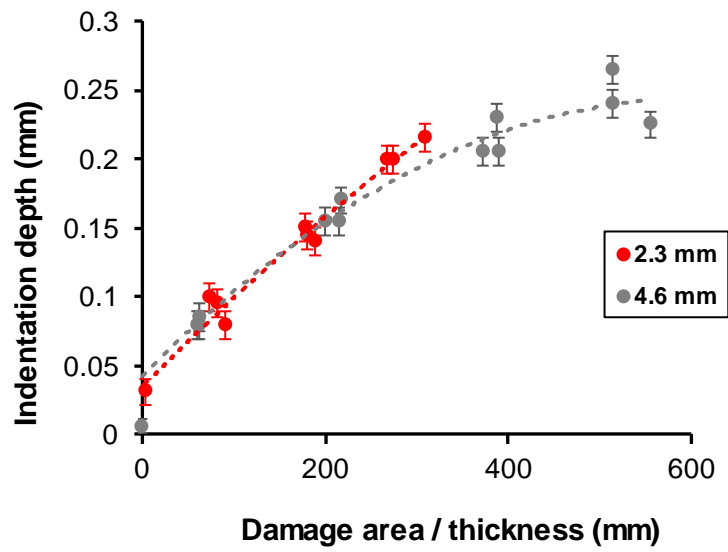


Figure 13. The indentation depth versus normalised interlaminar damage area (i.e. damage area divided by thickness) for the CF/Epoxy composite panels.

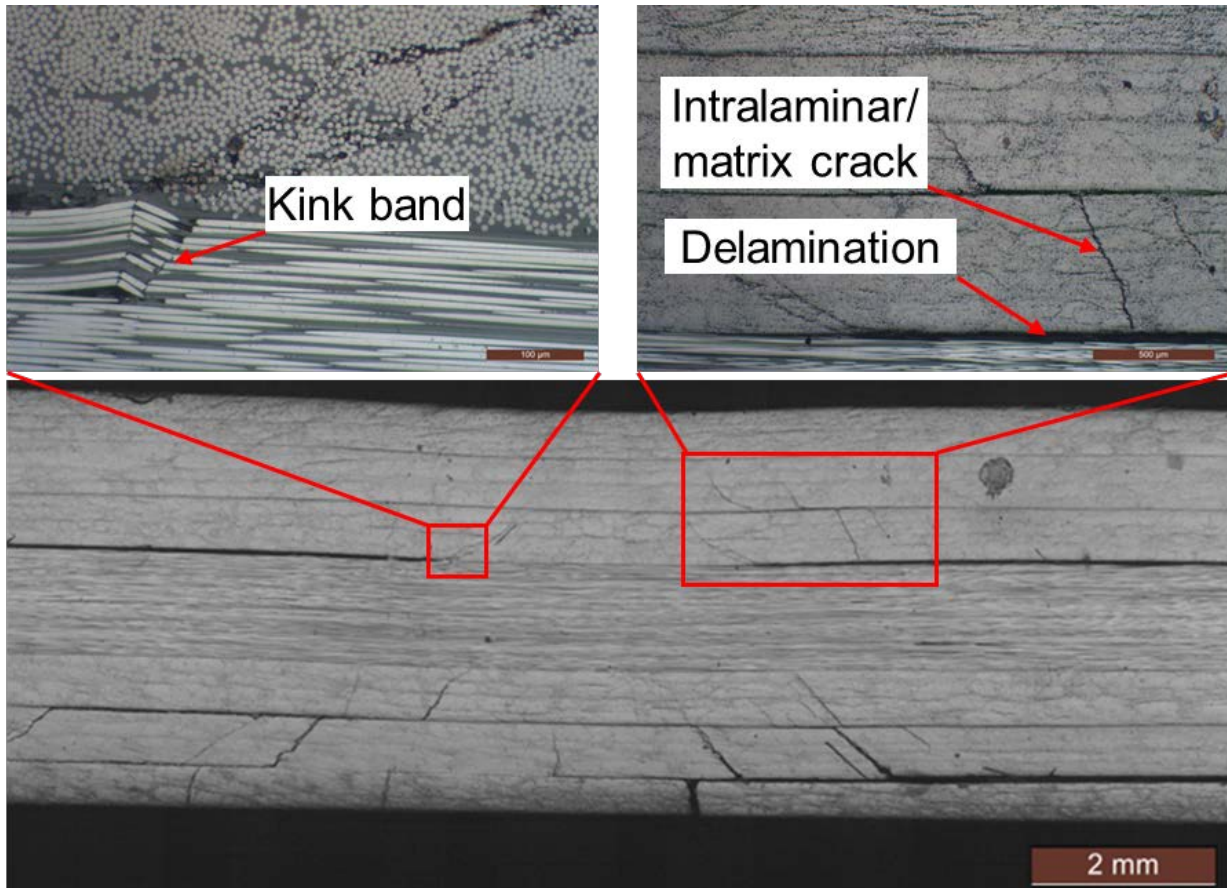


Figure 14. Optical microscopy images of a 4.6 mm thick CF/Epoxy composite panel after an impact of 15 J. (Showing a cross-section cut from the panel after grinding and polishing. The scale bars in the upper-left and upper-right micrographs represent 100  $\mu\text{m}$  and 500  $\mu\text{m}$ , respectively.)

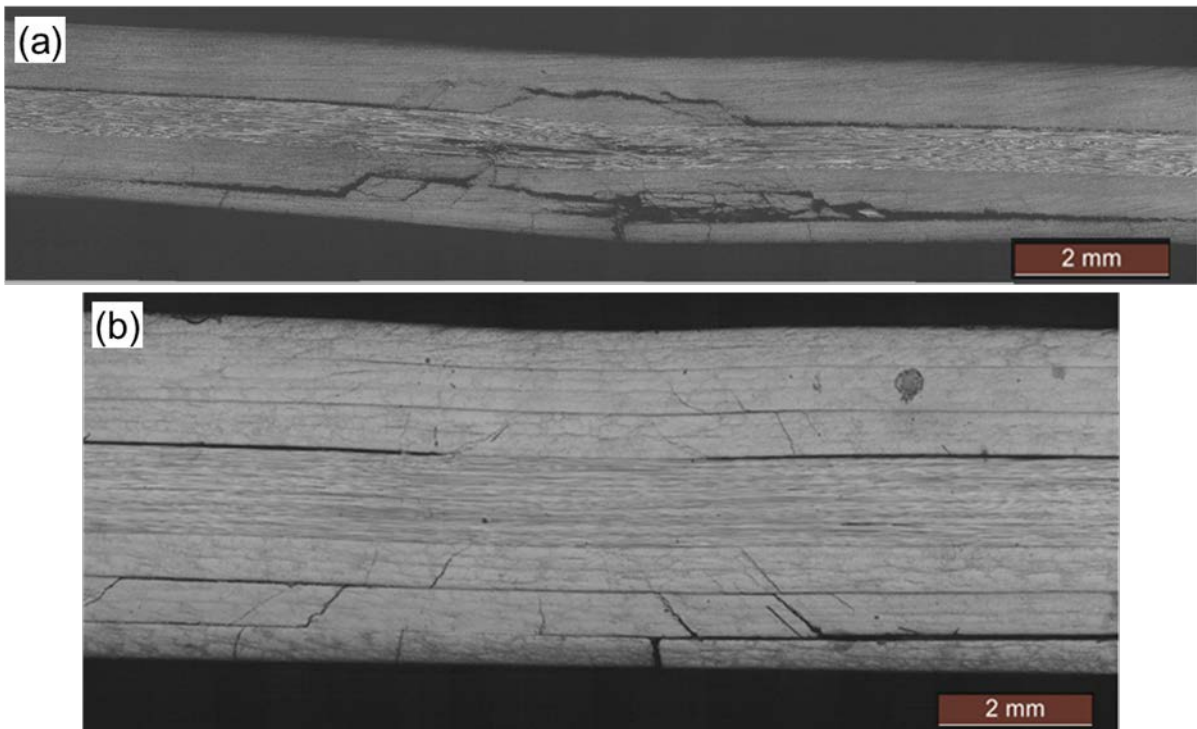


Figure 15. Optical microscopy images of (a) a 2.3 mm and (b) a 4.6 mm thick CF/Epoxy composite panel after an impact at 15 J. (Showing a cross-section cut from the panel after grinding and polishing.)